Ising ferromagnet on a fractal family: Thermodynamical functions and scaling laws

José Arnaldo Redinz and Aglaé C. N. de Magalhães
Centro Brasileiro de Pesquisas Físicas, Conselho Nacional de Desenvolvimento Científico e Tecnológico, rua Dr. Xavier Sigaud, 150, 22290-180, Rio de Janeiro, Brazil
(Received 26 August 1994)

The Ising model with external magnetic field on infinitely ramified fractal lattices is studied. We derive exact expressions for the specific heat, spontaneous magnetization, and susceptibility. The critical exponents α, β, and γ corresponding to these respective thermal functions (at zero field) as well as the correlation length critical exponent ν are obtained. The hyperscaling law extended to fractals and the Rushbrooke scaling law are verified for these fractals.

I. INTRODUCTION

After the work of Gefen, Mandelbrot, and Aharony[1] about criticality of the Ising model on several fractal lattices, there has been a lot of interest in the study of spin models on fractals and, in particular, on hierarchical lattices (HL) (see, for example, Ref. 2, and references therein). Many classical spin models, such as the Ising and Potts models, defined on HL constitute a class of exactly solvable models which can provide simple examples of interesting behaviors, like continuously varying critical exponents, phase transitions without true long-range order, etc., whose study in exactly solvable models on Bravais lattices has usually demanded quite a lot of effort and mathematical skill. Furthermore, a subclass of these models on HL can be considered approximations for the same models on Bravais lattices (see, e.g., Ref. 3).

The exactly solvable models with finite and short-range interactions defined on fractals which exhibit phase transitions at non-null temperature occur solely in *bond* HL's, i.e., two-rooted HL's, except the one introduced in Ref. 2, which refers to a three-rooted HL. In this cited paper there were proposed families of deterministic fractals, namely the m-sheet Sierpinski gaskets with side b [noted $(m\mathrm{SG})_b$], which have different fractal dimensions $d_f^{(m)}$ and on which the q-state Potts model can be exactly solved. In particular, concerning the Ising ferromagnet on the $(m\mathrm{SG})_2$, they obtained the exact critical temperature $T_c(m)$ showing that it becomes zero only in the finitely ramified case, i.e., in the standard Sierpinski gasket ($m=1$). However, the calculation of other physical quantities in this family of systems, such as the specific heat, magnetization, and susceptibility has not, in our knowledge, been done. Herein we derive exact expressions for these thermodynamical functions and we calculate their corresponding critical exponents α, β, and γ, as well as the correlation-length critical exponent ν. The evaluation of these critical exponents allows us to test the hyperscaling law extended to fractals (i.e., $d_f\nu=2-\alpha$) and the Rushbrooke scaling law ($\alpha+2\beta+\gamma=2$). The former one has been numerically verified in a number of HL (Refs. 4–6) and has been proved analytically[7] for the three-state antiferromagnetic Potts model on a diamond-type HL family. Concerning the Rushbrooke scaling law, there is much less evidence in favor of its validity on fractal systems. It has been tested[8] in the Potts ferromagnet on the Wheatstone-bridge HL using approximate methods in the derivation of β and γ; a slight violation of it for all values of the number of states q has been found, except for the Ising case ($q=2$). As far as we know, there is neither proof nor any reliable verification (in the sense of deriving exponents from exact expressions, at least, for their corresponding thermal functions) of the mentioned scaling law for spin models on fractals—a fact which could shed some light on the question of universality (see, for example, Refs. 9 and 10) in these systems. Herein, we verify this scaling law, as well as the hyperscaling law, for the Ising ferromagnet on the $(m\mathrm{SG})_2$ fractal family. Furthermore, we calculate in an exact way the order parameter associated with three-spin interactions (on alternate triangles only) and its corresponding susceptibility, and we verify that their critical exponents are equal to β and γ, respectively.

The outline of the paper is as follows. In Sec. II we define the Ising model on the $(m\mathrm{SG})_2$ lattice and derive recursive equations for the renormalization-group (RG) variables. In Sec. III we obtain the exact expressions for the following thermodynamical functions: specific heat, magnetization, susceptibility, the three-spin interaction order parameter, and its susceptibility. In Sec. IV we calculate their respective critical exponents and test the validity of the hyperscaling law and of the Rushbrooke scaling law. Finally the conclusions are given in Sec. V.

II. MODEL, RG EQUATIONS, AND CRITICAL FRONTIER

The $(m\mathrm{SG})_b$ (Ref. 2) is a generalization of the two-dimensional case of the SG family of Hilfer and Blumen.[11] Herein we will be interested only in the case $b=2$ of the $(m\mathrm{SG})_b$, which we shall refer to as simply mSG. This is constructed as follows for a fixed m: one starts with a triangle (level $n=0$) which is replaced by a basic cell (or generator) constituted of m triangular sheets connected only at the external vertices A, B, and C, each of which contains three smaller upward oriented triangles. The n level is obtained from the previous one by replacing each upward oriented triangle by the basic cell. This

recursive procedure is illustrated in Fig. 1 for $m=2$.

In the $n\to\infty$ limit one obtains a lattice with fractal dimension

$$d_f^{(m)}=\frac{\ln(3m)}{\ln 2}\ , \tag{1}$$

which has, unlike the finitely ramified SG($m=1$), an infinite order of ramification.[2] Notice that different values of m correspond to different fractals and we shall suppose, hereafter, that all the following calculations are done for a fixed m.

At each vertex of the mSG let us associate an Ising spin variable, $\sigma_i=\pm 1$, and consider the following model described by the dimensionless Hamiltonian:

$$-\beta\mathcal{H}=K_2\sum_{\langle ij\rangle}\sigma_i\sigma_j+K_3\sum_{\triangle}\sigma_i\sigma_j\sigma_k+h\sum_i z_i\sigma_i\ , \tag{2}$$

where $\beta\equiv 1/k_BT$, $K_2\equiv\beta J_2$, $K_3\equiv\beta J_3$, and $h\equiv\beta H$; J_2 is the coupling constant between nearest-neighbor pairs, J_3 is the three-body coupling among the spins at the vertices of an upward oriented triangle, and H is the external magnetic field. The three above respective sums are over all the first neighbors $\langle ij\rangle$, over the upward triangles $\triangle$, and over all the sites i of the mSG lattice; z_i stands for the coordination number of the site i.

This Hamiltonian is closed (no more couplings among the spins are generated) and form-invariant under our renormalization-group transformations. The three-body term is naturally generated by the one-body term after one renormalization step. The presence of the coordination number z_i in the field term asserts the Hamiltonian form invariance.[12,13] Notice also that the Hamiltonian (2) is invariant under spin reversal and change of sign of the odd terms, namely,

$$\mathcal{H}(\{\sigma_i\},K_2,K_3,h)=\mathcal{H}(\{-\sigma_i\},K_2,-K_3,-h)\ . \tag{3}$$

The procedure adopted herein for deriving the free energy follows along the lines of the one used by Bleher and Zalys[14] for the Ising model on diamond-type hierarchical lattices. We start, thus, defining the constrained partition functions at the n level by

$$W_n(s_A,s_B,s_C)=\mathrm{Tr}'\exp\{-\beta\mathcal{H}_n\}\quad(s_A,s_B,s_C=\pm 1), \tag{4}$$

where Tr′ stands for the trace over all configurations of the internal spins with the three rooted ones, σ_A, σ_B, and σ_C (see Fig. 1), fixed at the states s_A, s_B, and s_C, respectively. Hereafter we will use the abbreviated notation: $W_{an}=W_n\ (1,1,1)$, $W_{bn}=W_n\ (-1,-1,-1)$, $W_{cn}=W_n\ (1,1,-1)$, and $W_{dn}=W_n\ (-1,-1,1)$.

The recursive procedure of the mSG construction leads to recurrent equations relating the restricted partition functions at different levels, namely

$$\begin{aligned}W_{an+1}&=(W_{an}^3+3W_{an}W_{cn}^2+3W_{cn}^2W_{dn}+W_{dn}^3)^m\ ,\\ W_{cn+1}&=(W_{an}^2W_{cn}+W_{cn}^3+2W_{an}W_{cn}W_{dn}+2W_{cn}W_{dn}^2\\ &\quad+W_{bn}W_{cn}^2+W_{bn}W_{dn}^2)^m\ ,\end{aligned} \tag{5}$$

which reduce, for $m=1$, to Eqs. (11) of Liu.[15] Since our RG preserves the Hamiltonian symmetry (3), the equations for W_{bn+1} and W_{dn+1} can be obtained from the above ones by spin reversal, i.e., interchanging a and b, as well as c and d. The initial conditions for these equations corresponding to the Boltzmann weights of the triangle ($n=0$ in Fig. 1) are given by

$$W_{a0}=e^{3K_2+K_3+6h}\ ,\quad W_{c0}=e^{-K_2-K_3+2h}\ , \tag{6}$$

while those for W_{b0} and W_{d0} can be obtained through the invariance of the Hamiltonian [Eq. (3)].

Introducing the relative variables

$$\begin{aligned}p_n&=\left[\frac{W_{dn}W_{bn}}{W_{an}W_{cn}}\right]^{1/2}\ ,\quad y_n=\left[\frac{W_{bn}}{W_{an}}\right]^{1/2}\ ,\\ t_n&=\left[\frac{W_{cn}W_{dn}}{W_{an}W_{bn}}\right]^{1/2}\ ,\end{aligned} \tag{7}$$

one can derive, from (5), recurrent equations for p_n, y_n, and t_n (whose expressions we shall omit since they are quite long), which define our RG transformation $\mathcal{R}:\{p_n,y_n,t_n\}\to\{p_{n+1},y_{n+1},t_{n+1}\}$. The corresponding initial conditions for our RG variables are

$$p_0=e^{-8h}\ ,\quad y_0=e^{-6h-K_3}\ ,\quad t_0=e^{-4K_2}\ . \tag{8}$$

Successive iterations of $\mathcal{R}$ subjected to the above initial conditions lead to critical frontiers and phase attractors in the (p,y,t) space. We shall restrict ourselves to the

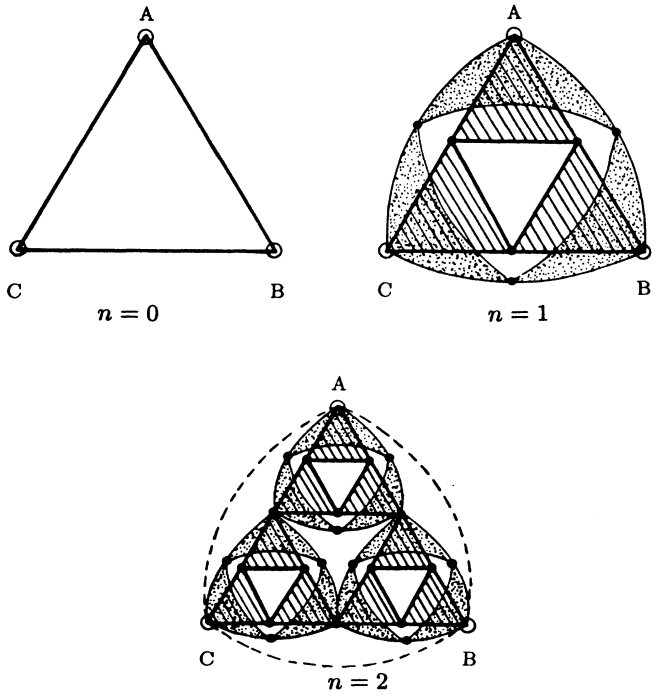

FIG. 1. The three first steps of construction of the two-sheet mSG fractal lattice. For better visualization, we have represented the second sheet of the $n=2$ level connected to the external sites A, B, and C by just a single dashed curve.

case of positive K_2, K_3, and h, which implies that each of the RG variables is confined to the interval [0,1]. This restriction is due to the fact that there is no preservation of the antiferromagnetic ground state in our RG when K_2 is negative.[2] The axes $(1,y,1)$ and $(1,1,t)$, as well as the line $(p,p^{3/4},1)$, are invariant under the RG transformation $\mathcal{R}$.

In the $m=1$ case the line $(p,p^{3/4},1)$, corresponding to the noninteracting spins subjected to a magnetic field, results, as an artifact of the decimation, in a line of fixed points.[16] For the $m>1$ case, all the points in this line, with exception of the fixed point (1, 1, 1), are successively renormalized towards the (0, 0, 1) attractor.

In the $(1,1,t)$ axis, which corresponds to the usual Ising model with $J_3=H=0$, our RG transformation reduces to

$$t_{n+1}=\left[\frac{t_n(1+3t_n)}{1-t_n+4t_n^2}\right]^m , \tag{9}$$

which agrees with Eq. (22) of Ref. 2 and recovers, for $m=1$, Eq. (1) of Ref. 1. Equation (9) (with $m>1$) has three fixed points in the $0\le t\le 1$ interval, namely the two attractors $t=0$ and $t=1$, corresponding to the ferromagnetic ($T=0$) and paramagnetic ($T=\infty$) phases, respectively, and the unstable critical point $t_c^{(m)}$ separating these two phases. Typical values of $t_c^{(m)}$ are $t_c^{(1)}=0$, $t_c^{(2)}=0.309\ldots$, $t_c^{(3)}=0.433\ldots$, and $t_c^{(4)}=0.513\ldots$. In Fig. 2 we show the plot of k_BT_c/J_2 as a function of the fractal dimension d_f (upper curve). The plot starts with infinite derivative at $d_f=\ln(3)/2$ ($m=1$) and behaves asymptotically as 2^{d_f} for $d_f\to\infty$, similar to the case of the Potts ferromagnet on d-dimensional Migdal-Kadanoff HL types[17] (where $d_f=d$). This exponential behavior is in contrast to the behavior $k_BT_c/J_2\sim 2d$ found for the Ising ferromagnet on large d-dimensional hypercubical lattices.[18]

In the $(1,y,1)$ axis, which corresponds to the Ising model with solely three-spin interactions on upward triangles ($J_2=H=0$), the RG transformation becomes

$$y_{n+1}=\left[\frac{y_n^2(3+y_n^4)}{1+3y_n^4}\right]^{m/2} , \tag{10}$$

which reduces, for $m=1$, to Eq. (2.35) of Ref. 16. In the case $m>1$, Eq. (10) presents three fixed points: the two attractors $y=0$ (at $T=0$) and $y=1$ (at $T=\infty$) corresponding, respectively, to the ordered and the paramagnetic phases, and the unstable one $y_c^{(m)}$ separating these two basins of attraction. Typical values of $y_c^{(m)}$ are $y_c^{(1)}=0$, $y_c^{(2)}=0.346\ldots$, $y_c^{(3)}=0.485\ldots$, and $y_c^{(4)}=0.557\ldots$, and k_BT_c/J_3 as function of d_f is shown in Fig. 2 (lower curve) exhibiting an asymptotic behavior as $2^{d_f/2}$ for large d_f.

We have verified that, for any value of $m>1$, apart from the axis $(1,y,1)$ and $(1,1,t)$, all points in the considered cube are successively renormalized into the (0,0,1) attractor corresponding to the paramagnetic phase (with $h\to\infty$). Therefore, the magnetic field as well as the three-spin interactions destroy the para-ferromagnetic transition of the usual Ising model on the mSG ($m>1$).

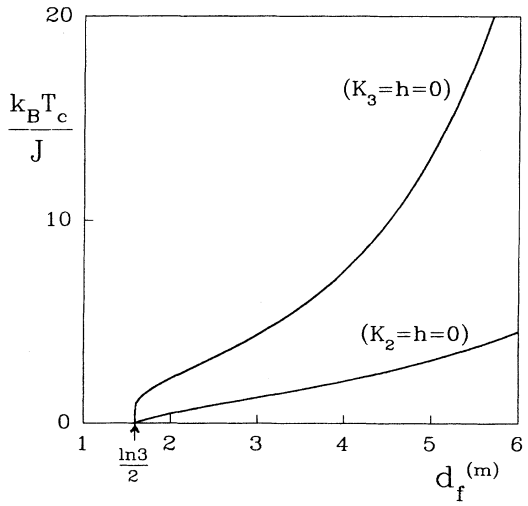

FIG. 2. The critical temperature T_c as a function of the fractal dimension $d_f^{(m)}$. In the upper (lower) curve we show the critical points of the Ising model $K_3=h=0$ ($K_2=h=0$).

III. THERMODYNAMICAL FUNCTIONS

In this section we calculate the exact expressions for the specific heat, magnetization, susceptibility, the three-spin interaction order parameter, and its corresponding susceptibility, of the Ising model on the mSG. For this, we shall first derive the free energy in terms of the set of RG variables (p,y,t).

The partition function of the model at the n level is given by

$$Z_n=W_{an}+W_{bn}+3W_{cn}+3W_{dn}=W_{an}g_n , \tag{11}$$

where

$$g_n=1+y_n^2+3\frac{y_n^2t_n}{p_n}+3p_nt_n . \tag{12}$$

On the other hand, W_{an} satisfies [see Eq. (5)] the following recursive relation:

$$W_{an}=W_{an-1}^{3m}v_{n-1}^m , \tag{13}$$

where

$$v_n=1+3\left[\frac{y_n^2t_n}{p_n}\right]^2+3\frac{y_n^4t_n^3}{p_n}+(p_nt_n)^3 . \tag{14}$$

Successive iterations of Eq. (13) combined with Eq. (11) leads to

$$Z_n=W_{a0}^{(3m)^n}g_n\prod_{i=0}^{n-1}v_i^{m(3m)^{n-1-i}} . \tag{15}$$

Taking into account that the function g_n is bounded in the case of finite h ($p_n\neq 0$), the dimensionless free energy per site f_{sn} at the n level ($n\gg 1$) is given by

$$f_{sn} \equiv -\frac{\ln Z_n}{N_{sn}} = \frac{(1-3m)}{3m}\left[3K_2+6h+K_3+\frac{1}{3}\sum_{i=0}^{n-1}(3m)^{-i}\ln v_i\right], \tag{16}$$

where the number of sites N_{sn} at the n level is

$$N_{sn}=3m\frac{(3m)^n-1}{3m-1}+3 . \tag{17}$$

The dimensionless internal energy U_n of the usual Ising model ($H=J_3=0$) at the n level ($n \gg 1$) can be obtained by

$$U_n \equiv \frac{\langle \mathcal{H}_n \rangle}{J_2 N_{sn}}\bigg|_{h=K_3=0} = \frac{\partial f_{sn}}{\partial K_2}\bigg|_{h=K_3=0} = \frac{(1-3m)}{3m}\left[3-\frac{4}{3}t_0\sum_{i=0}^{n-1}(3m)^{-i}\left[\frac{6t_i+12t_i^2}{1+3t_i^2+4t_i^3}\right]\times\prod_{j=1}^{i} r_j\right], \tag{18}$$

where the symbol $\langle\ \rangle$ stands for the thermal average on the mSG at the n level, and where $r_j \equiv (\partial t_{j+1}/\partial t_j)|_{t_j}$. The dimensionless specific heat per site C_n at the n level can be calculated through derivation of U_n, namely $C_n=\partial U_n/\partial(1/K_2)$. In Fig. 3 we show the specific heats for the cases $m=1$ (the SG), 2, 3, and 4. Note that in the horizontal axis we used, for ease of representation, the variable $x \equiv e^{-4K_2/m}$. None of them diverges at the critical temperature indicating, thus, negative values for the α exponents (their explicit values will be given in the next section) similar to the results found for the usual Ising model on a variety of bond hierarchical lattices.[13,4,5] The $m=2$ case has a cusplike behavior with a finite peak at $x_c^{(2)}$. The other cases with $m>2$ present rounded peaks localized below the critical points $x_c^{(m)}$, similar to the behavior found in some systems with infinitely degenerate ground states (see Ref. 7 and references therein).

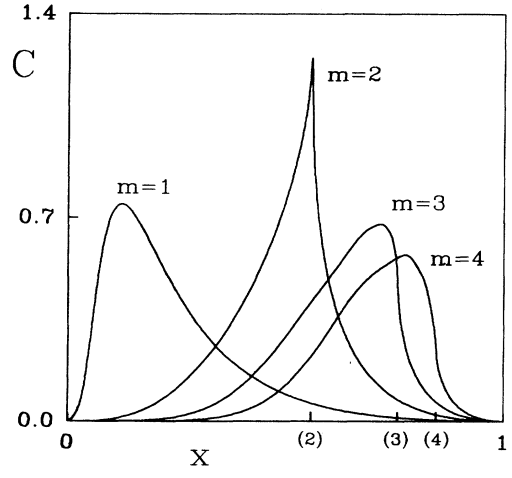

FIG. 3. The dimensionless specific heats per site as functions of the variable $x=e^{-4K_2/m}$ for the cases $m=1$, 2, 3, and 4 at the $n=30$ level. The tick marks labeled (2), (3), and (4) correspond to the critical temperatures $t_c^{(2)}$, $t_c^{(3)}$, and $t_c^{(4)}$, respectively.

Due to the introduction of the coordination number z_i in the field term of the Hamiltonian we shall define the magnetization M at the n level by

$$M_n \equiv \frac{\sum_i z_i^{(n)}\langle\sigma_i\rangle}{\sum_i z_i^{(n)}} = -\left[\frac{N_{sn}}{N_{cn}}\right]\frac{\partial f_{sn}}{\partial h}\bigg|_{h=K_3=0}, \tag{19}$$

where the sums are over all the sites of the mSG at the n level, and where we introduced $N_{cn} \equiv \sum_i z_i^{(n)}$ in order to normalize the magnetization M_n at $T=0$.

From Eqs. (16) and (19) we obtain that

$$M_n = 1+D_n(\{t_i\},\{a_i\},\{b_i\}) , \tag{20}$$

with

$$D_n(\{t_i\},\{a_i\},\{b_i\}) = \frac{1}{3}\sum_{i=0}^{n-1}(3m)^{-i}\left\{\frac{t_i^2[2(1+t_i)a_i-b_i]}{1+3t_i^2+4t_i^3}\right\}, \tag{21}$$

where we have defined $a_i \equiv (\partial y_i/\partial h)|_{h=K_3=0}$ and $b_i \equiv (\partial p_i/\partial h)|_{h=K_3=0}$. In this calculation we have taken into account that, for any value j,

$$\frac{\partial t_j}{\partial h}\bigg|_{h=K_3=0}=0 , \tag{22}$$

which one can derive as a consequence of the Hamiltonian symmetry [Eq. (3)].

The functions a_i and b_i introduced in (21) obey the following recurrent equations:

$$\begin{aligned} a_{i+1} &= m\left[\frac{3(1-t_i)}{1-t_i+4t_i^2}\right]a_i + m\left[\frac{6t_i^2}{(1-t_i+4t_i^2)(1+t_i)}\right]b_i , \\ b_{i+1} &= m\left[\frac{4(1+t_i-t_i^2-t_i^3)}{(1-t_i+4t_i^2)(1+3t_i)}\right]a_i + m\left[\frac{1-2t_i+13t_i^2+4t_i^3}{(1-t_i+4t_i^2)(1+3t_i)}\right]b_i , \end{aligned} \tag{23}$$

with the initial conditions $a_0=-6$ and $b_0=-8$. The plots of magnetization for the cases $m=2$, 3, and 4 are shown in Fig. 4 by solid lines.

As we have seen in the previous section, J_3 plays the same role as H in what concerns the para-ferromagnetic transition of the usual Ising model, i.e., both destroy this transition. We can, thus, introduce the following order parameter $M_\triangle$ conjugated to the three-spin coupling J_3:

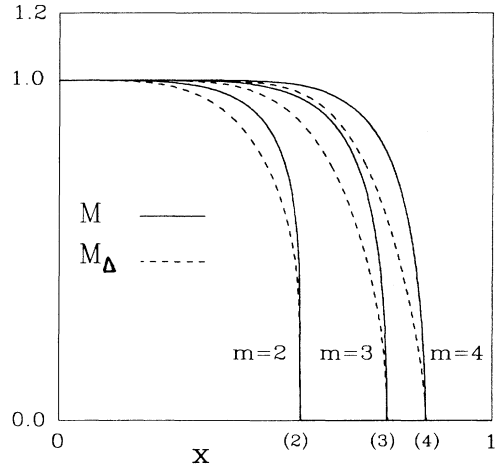

FIG. 4. The spontaneous magnetizations M (solid lines) and the function $M_\triangle$ (dashed lines) as functions of x for the cases $m=2$, 3, and 4 at the $n=30$ level. The numbers in parenthesis (2), (3), and (4) correspond to the critical temperatures $t_c^{(2)}$, $t_c^{(3)}$, and $t_c^{(4)}$, respectively.

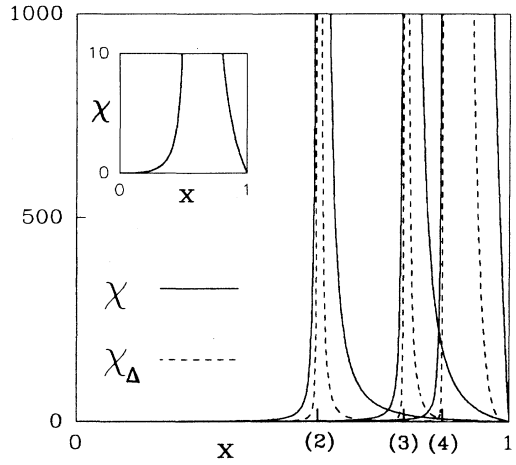

FIG. 5. The dimensionless susceptibilities χ (solid lines) and $\chi_\triangle$ (dashed lines) as functions of x for the cases $m=1$, 2, and 3 at the $n=30$ level. The tick marks labeled (2), (3), and (4) correspond to the critical temperatures $t_c^{(2)}$, $t_c^{(3)}$, and $t_c^{(4)}$, respectively. The inset shows a detail of the susceptibility χ for the case $m=2$.

$$M_\triangle = \lim_{n\to\infty} M_{\triangle n} , \tag{24}$$

with $M_\triangle$ at the n level being given by

$$M_{\triangle n} \equiv \frac{\sum_{\triangle} \langle \sigma_i \sigma_j \sigma_k \rangle}{N_{\triangle n}} , \tag{25}$$

where the sum is over all the $N_{\triangle n}$ upward-oriented triangles at the n level mSG. $N_{\triangle n}$ was introduced in order to normalize $M_\triangle$ at $T=0$.

$M_{\triangle n}$ can be calculated from f_{sn} [Eq. (16)] through

$$M_{\triangle n} = -\left[\frac{N_{sn}}{N_{\triangle n}}\right] \frac{\partial f_{sn}}{\partial K_3}\bigg|_{h=K_3=0} , \tag{26}$$

and we have obtained a functional form similar to that of M [Eq. (20)], namely,

$$M_{\triangle n} = 1 + 6 D_n(\{t_i\},\{A_i\},\{B_i\}) , \tag{27}$$

where $A_i \equiv (\partial y_i / \partial K_3)|_{h=K_3=0}$ and $B_i \equiv (\partial p_i / \partial K_3)|_{h=K_3=0}$ satisfy the same recurrent equations as those of a_i and b_i [Eq. (23)], but with different initial conditions ($A_0=-1$ and $B_0=0$).

The plots of $M_{\triangle n}$ for the cases $m=2$, 3, and 4 are shown in Fig. 4 (in dashed lines). From this figure one confirms that $M_\triangle$ plays the role of an order parameter since it vanishes above a critical temperature and, as we have already seen, the application of its conjugated field (J_3), no matter how small it may be, destroys the phase transition. Notice also that M and $M_\triangle$ become null at the *same* critical temperature $t_c^{(m)}$. Furthermore, as we will see in the next section, both order parameters, as well as their corresponding susceptibilities, have the same critical exponents (i.e., $\beta^{(m)}=\beta_\triangle^{(m)}$ and $\gamma^{(m)}=\gamma_\triangle^{(m)}$) for any given value of m. This can be understood by noticing that the addition of either a small magnetic field H or a three-spin interaction J_3 to the two-spin interaction Ising model breaks the same symmetry [i.e., the $Z(2)$ one]. A similar fact occurred in the Ising model with solely three-spin interactions on the triangular lattice,[19] where both the magnetic field and the two-spin interaction break the symmetry under the reversal of all spins on any two of the three sublattices. These sublattices are constructed such that the three-spin interaction involves a site from each sublattice.

The zero-field susceptibility $\chi_n \equiv (\partial M_n / \partial H)|_{h=K_3=0}$ at the n level is linked to f_{sn} through

$$J_2 \chi_n = -\left[\frac{N_{sn}}{N_{cn}}\right] K_2 \frac{\partial^2 f_{sn}}{\partial h^2}\bigg|_{h=K_3=0} , \tag{28}$$

and can be obtained analytically from (16). In Fig. 5 we show the plots of susceptibility in the cases $m=2$, 3, and 4. The susceptibilities diverge only at the critical temperatures, unlike that of the Ising model on the diamond hierarchical lattice,[14] where there is a divergence for all $t > t_c$. Similarly we define for the function $M_{\triangle n}$ the zero-three-spin interaction susceptibility $\chi_{\triangle n} \equiv (\partial M_{\triangle n} / \partial J_3)|_{h=K_3=0}$, which can be obtained from (16). The plots of $\chi_\triangle$ for $m=2$, 3, and 4 are shown in Fig. 5 (in dashed lines). This susceptibility presents a divergence at the critical temperature $t_c^{(m)}$, similarly to the susceptibility χ.

IV. CRITICAL EXPONENTS AND SCALING LAWS

In this section we obtain the critical exponents ν, α, β, and γ corresponding to the respective critical behaviors of the correlation length, specific heat, spontaneous magnetization, and susceptibility for the usual Ising model ($K_3=h=0$). With these exponents we test the validity of

the hyperscaling as well as of the Rushbrooke scaling law.

Linearization of (9) in the neighborhood of the critical point $t_c^{(m)}$ leads to

$$\nu^{(m)}=\frac{\ln 2}{\ln r_c^{(m)}} , \tag{29}$$

where $r_c^{(m)}\equiv(\partial t_{n+1}/\partial t_n)|_{t_c^{(m)}}$, which gives the exact results for the correlation length critical exponents $\nu^{(2)}=0.928\ldots$, $\nu^{(3)}=0.850\ldots$, $\nu^{(4)}=0.840\ldots$, etc. (see Fig. 6 for ν as function of the fractal dimension $d_f^{(m)}$).

The plots shown in Figs. (3), (4), and (5) of the thermal quantities were calculated for the mSG with n set to 30, which correspond to approximately $N_{sn}^{(m)}\simeq(3m)^{30}$ spins ($N_{sn}^{(1)}\simeq 10^{14}$, $N_{sn}^{(4)}\simeq 10^{32}$). The analysis of the convergence of these functions with increasing n shows that this size provides numerical values for C_n, M_n, $M_{\triangle n}$, χ_n, and $\chi_{\triangle n}$ (with exception for χ_n and $\chi_{\triangle n}$ in the neighborhood of $t_c^{(m)}$), which do not vary up to the 16th decimal place if we increase n. We shall, therefore, consider that C_{30}, M_{30}, $M_{\triangle 30}$, χ_{30}, and $\chi_{\triangle 30}$ are very good approximations for their corresponding quantities in the thermodynamical limit.

Using the exact expression of C_n derived from (18) we obtained from a log-log plot of $C_{30}(t)-C_{30}(t_c^{(m)})$ versus $(t-t_c^{(m)})$ the following values for the specific-heat exponents $\alpha^{(m)}$: $\alpha^{(2)}\simeq -0.401$, $\alpha^{(3)}\simeq -0.696$, $\alpha^{(4)}\simeq -1.012$, etc. . . (see the plot of α versus $d_f^{(m)}$ in Fig. 6).

The log-log plots of $M_{30}(t)$ versus $(t-t_c^{(m)})$ led to the following values for the magnetization exponents $\beta^{(m)}$: $\beta^{(2)}\simeq 0.247$, $\beta^{(3)}\simeq 0.441$, $\beta^{(4)}\simeq 0.582$, etc. . . (see its variation with $d_f^{(m)}$ in Fig. 6). Using a similar procedure we verified that the function $M_{\triangle n}$ vanishes in the same critical temperature $t_c^{(m)}$ with the same exponent $\beta^{(m)}$ calculated for the magnetizations M_n.

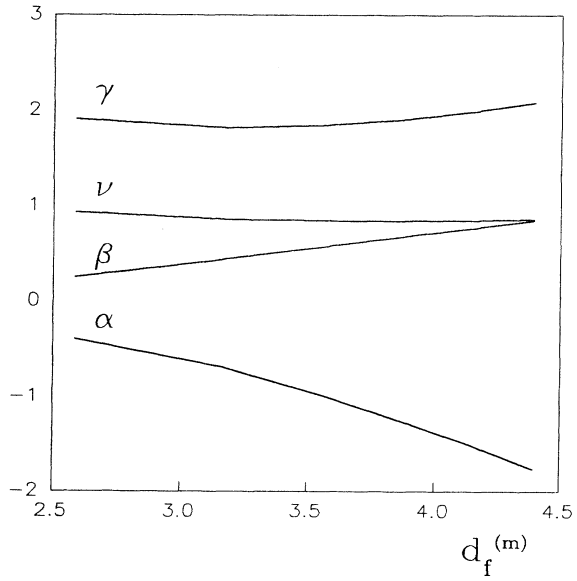

FIG. 6. The critical exponents ν, α, and γ of the zero-field Ising model on the mSG as functions of the fractal dimension $d_f^{(m)}$.

In the case of the critical exponents $\gamma^{(m)}$ we shall calculate them through finite size scaling (FSS) (see, for example, Ref. 20), since the susceptibilities $\chi^{(m)}$ vary in a very steep way with small deviations of $t_c^{(m)}$ generating, thus, large numerical errors in the determination of $\gamma^{(m)}$ through a log-log plot of $\chi^{(m)}$ versus $(t-t_c^{(m)})$. For a given m and increasing values of n, we observe that the maximum of $\chi_n^{(m)}$ increases with n tending to diverge in the thermodynamical limit. This peak occurs at the pseudocritical temperature $t_{pcn}^{(m)}$ which converges, as n increases, to the critical temperature $t_c^{(m)}$ as

$$|t_{pcn}^{(m)}-t_c^{(m)}|\sim L_n^{-1/\theta^{(m)}} \quad (n\gg 1) , \tag{30}$$

where L_n is the linear size of the n-level mSG ($L_n=2^n$) and $\theta^{(2)}\simeq 0.928$, $\theta^{(3)}\simeq 0.850$, $\theta^{(4)}\simeq 0.839$, etc. . . . These values of $\theta^{(m)}$ coincide with the exact ones of the critical exponents $\nu^{(m)}$ with excellent agreement (with relative errors of order 0.1%), which corroborate the fact that the equality $\theta=\nu$ seems to be usually true within the FSS theory.

The scaling for the susceptibility at finite levels ($n\gg 1$) of the mSG is given, according to the FSS theory, by

$$\chi_n(t_{pcn})\sim L_n^{\gamma^{(m)}/\nu^{(m)}} \quad (n\gg 1) , \tag{31}$$

which led to the upper curve shown in Fig. 6, in particular, $\gamma^{(2)}\simeq 1.904$, $\gamma^{(3)}\simeq 1.814$, $\gamma^{(4)}\simeq 1.847$, etc. . . . The values of $\gamma^{(m)}$ obtained directly from a log-log plot of χ_{30} versus $(t-t_c^{(m)})$ agree with these one up to the second decimal place. Applying a similar procedure for the susceptibility $\chi_{\triangle n}$ we obtained the same set of $\gamma^{(m)}$ exponents corresponding to the susceptibilities χ_n.

The hyperscaling extended to fractal systems, namely

$$d_f\nu=2-\alpha , \tag{32}$$

although has not been proved in general, has been exactly verified in a number of systems defined on several fractals.[4–7] Here, using the exact ν exponent derived from Eq. (29), the mSG fractal dimension given by (1), and the above approximate $\alpha^{(m)}$ exponents, we obtained that $d_f^{(2)}\nu^{(2)}+\alpha^{(2)}\simeq 1.998$, 2.001 (for $m=3$), 1.999 (for $m=4$), etc. . . .

Concerning the test of the Rushbrooke scaling law, we obtained that $\alpha^{(m)}+2\beta^{(m)}+\gamma^{(m)}\simeq 1.997$, 2.000, and 1.999 for $m=2$, 3, and 4, respectively. This law has also been checked[8] for the Ising ferromagnet on the Wheatstone-bridge hierarchical lattice using approximate methods in the determination of the thermal quantities and their respective critical exponents.

V. CONCLUSIONS

We have presented an exactly solvable model on a family of deterministic fractals, the ferromagnetic Ising model with external field and three-spin interactions on the m-sheet Sierpinski gasket fractals. The exact expressions for thermal physical quantities as functions of temperature in the case of the two-spin interaction Ising model

were obtained for different values of m and they present a very good convergence with increasing hierarchical level n.

We have verified that the function $M_{\triangle}$ defined in Eq. (24) can be used as an alternative order parameter in this plain Ising ferromagnet, since (i) it vanishes at the same critical temperature with the same critical exponent β as does the magnetization M; (ii) the application of its conjugated field (i.e., the three-spin interaction J_3), no matter how small it may be, destroys the paraferromagnetic transition; (ii) its corresponding susceptibility $\chi_{\triangle}$ diverges at the critical temperature with the same exponent γ as the susceptibility χ.

With the computed critical exponents ν, α, β, and γ, we tested the validity of the hyperscaling law and of the Rushbrooke scaling law. Despite the errors implicit in the numerical evaluations of the critical exponents (with exception of ν, which was calculated exactly), the values obtained herein give very good evidence in support of the validity of these laws for the Ising ferromagnet on the mSG fractal lattice family. In our knowledge, there has been no report in the literature concerning any proof or verification (without using approximate analytical expressions for the corresponding thermodynamical functions) of the Rushbrooke law on any fractal system.

ACKNOWLEDGMENTS

The authors would like to thank Constantino Tsallis, Rita M. Z. dos Santos, Evaldo M. F. Curado, and Francisco C. Alcaraz for helpful discussions on the subject. We also thank the financial support from the Brazilian agency Conselho Nacional de Desenvolvimento Científico e Tecnológico, CNPq.

[1]Y. Gefen, B. B. Mandelbrot, and A. Aharony, Phys. Rev. Lett. **45**, 855 (1980).
[2]F. S. de Menezes and A. C. N. de Magalhães, Phys. Rev. B **46**, 11 642 (1992).
[3]A. N. Berker and S. Ostlund, J. Phys. C **12**, 4961 (1979).
[4]C. Tsallis, J. Phys. C **18**, 6581 (1985).
[5]S. Coutinho, O. D. Neto, J. R. L. Almeida, E. M. F. Curado, and W. A. M. Morgado, Physica A **185**, 271 (1992).
[6]L. da Silva, E. M. F. Curado, W. A. M. Morgado, and S. Coutinho (unpublished).
[7]J. A. Redinz, A. C. N. de Magalhães, and E. M. F. Curado, Phys. Rev. B **49**, 6689 (1994).
[8]E. P. da Silva and C. Tsallis, Physica A **167**, 347 (1990).
[9]B. Hu, Phys. Rev. Lett. **55**, 2316 (1985).
[10]Y. K. Wu and B. Hu, Phys. Rev A **35**, 1404 (1987).
[11]R. Hilfer and A. Blumen, J. Phys. A **17**, L537 (1984).
[12]J. M. Yeomans and M. E. Fisher, Phys. Rev. B **24**, 2825 (1981).
[13]J. R. Melrose, J. Phys. A **16**, 3077 (1983).
[14]P. M. Bleher and E. Zalys, Commun. Math. Phys. **120**, 409 (1989).
[15]S. H. Liu, Phys. Rev. B **32**, 5804 (1985).
[16]J. H. Luscombe and R. C. Desai, Phys. Rev. B **32**, 1614 (1985).
[17]L. R. da Silva and C. Tsallis, J. Phys. A **20**, 6013 (1987).
[18]M. E. Fisher and D. S. Gaunt, Phys. Rev. **133**, A244 (1964).
[19]R. J. Baxter, M. F. Sykes, and M. G. Watts, J. Phys. A **8**, 245 (1975).
[20]M. N. Barber, in *Phase Transitions and Critical Phenomena*, edited by C. Domb and J. L. Lebowitz (Academic, New York, 1983), Vol. 8, p. 145.